ELSEVIER

Ceramics International 30 (2004) 901–910

CERAMICS INTERNATIONAL

www.elsevier.com/locate/ceramint

Brazing silicon nitride to an iron-based intermetallic using a copper interlayer

M. Brochu [a], M.D. Pugh [b], R.A.L. Drew [a,*]

[a] *Metals and Materials Engineering Department, McGill University, 3610 University Street, Montreal, Que., Canada H3A 2B2*
[b] *Mechanical Engineering Department, Concordia University, 1455 de Maisonneuve Blvd West, Montreal, Que., Canada H3G 1M8*

Received 5 September 2003; received in revised form 14 September 2003; accepted 10 October 2003

Available online 20 March 2004

Abstract

The effect of adding a copper interlayer to absorb the residual stresses produced during cooling of a silicon nitride (Si_3N_4) ceramic brazed to an iron aluminide alloy was demonstrated. Differential scanning calorimetry (DSC) results showed the positive influence of the copper interlayer in diluting the high-titanium content brazing alloy by decreasing the quantity of active brazing alloy (ABA) available for reaction. The reaction layer formation mechanism was investigated by low voltage line scan FESEM and was shown to consist of a growth competition between the TiN and Ti_5Si_3 layer. An activation energy of 137 kJ/mol for the reaction layer formation was calculated. A Fe/Cu–Ti alloy reaction at the interface between the Cu interlayer and the FA-129 was observed. This reaction zone extended up to 100 μm in thickness. The maximum bending strength obtained was 160 MPa. All fractures occurred at the Cu/Si_3N_4 interface, suggesting higher strengths for the FA-129/Cu interface.

Keywords: D. Si_3N_4; Brazing; Cu interlayer; Residual stress; FA-129

1. Introduction

High temperature strength, high hardness and corrosion resistance are properties which make ceramics suitable materials for severe applications. However, their brittleness combined with the difficulty in processing complex shapes have modified design concepts and joining simple shaped ceramic pieces to themselves or to metallic substrates has become a key technology [1]. In certain applications, the metallic component will absorb shocks or vibrations; the ceramic will only be exposed to the “aggressive” portion (thermal, chemical and wear for example). Among the advanced ceramics, silicon nitride (Si_3N_4) possesses outstanding properties for structural applications, such as high temperature strength, wear and corrosion resistance [2].

Intermetallic materials generally possess a mixture of atomic bonding; metallic combined with covalent or ionic, depending on the composition. Iron aluminides possess high temperature strength and excellent environmental resistance. However, their room temperature brittleness has limited their use. Alloying has shown tremendous effects on the room temperature ductility in air. For example, Cr-additions change the elongation from 2 to 6.4% without decreasing the yield strength when tested in air [3]. The FA-129 (15.9Al–5.5Cr–1.0Nb–0.05C–bal.Fe (wt.%)) is a DO_3 iron aluminide alloy developed by ORNL. This alloy was developed to exhibit high temperature strength with good room temperature ductility [4].

Brazing is one of the simplest joining processes, based on melting and solidification of an insert filler metal between the parent materials. Brazing of ceramics requires the addition of an active element into the filler metal to destabilize the covalent or ionic bond of the ceramic and form an intermediate reaction layer. This modification of the process is called reactive brazing. The most common active element used is titanium [5].

The major factor determining the strength of a metal/ceramic joint is the maximum tensile stress developed in the ceramic during cooling. Soft interlayers, such as Cu or Ni, have been proved to be successful in absorbing the detrimental stresses by plastic deformation [6]. Kim and Park [7] have studied the effect of residual stress absorption

* Corresponding author. Tel.: +1-514-398-1773; fax: +1-514-398-4492.
E-mail address: robin.drew@mcgill.ca (R.A.L. Drew).

0272-8842/$30.00
doi:10.1016/j.ceramint.2003.10.011

by a copper interlayer in the system Si_3N_4/Stainless Steel 316 as a function of the interlayer thickness. The optimum Cu thickness to reduce the effects of residual stress in their system was 200 μm. Thinner interlayers showed less plastic deformation, resulting in higher residual stresses in the ceramic and lower strength joints. Thicker interlayers have shown a slight reduction in mechanical strength, but remain higher than in the case of thinner interlayers (<200 μm).

Previous research work performed by the authors to directly braze Si_3N_4 to FA-129 was not successful as typical concave/convex fracture occurred from the edge of the ceramic body, independently of the brazing conditions used [8]. These results were explained by the high stress required to plastically deform the intermetallic alloy, as the yield stress ranges from 425 to 385 MPa between room temperature and 600 °C [9]. In another set of experiments, the effect of temperature on the microstructure of brazed joints using copper interlayers were done to determine the maximum possible brazing temperature for this system [10]. The results obtained have shown that for a brazing temperature higher than 1025 °C, major damage of the structure was obtained. Significant diffusion of Al from the intermetallic into the Cu interlayer occurred, melting the copper interlayer and actually pushing the molten Cu–Al outside of the joint. In addition, the Cu–Al liquid penetrates the FA-129 alloy producing a decohesion of the grain structure.

The objective of this research work was to study the effectiveness of a copper interlayer in accommodating the residual stresses produced during cooling between the Si_3N_4 and the FA-129. Reaction development, microstructural evolution and mechanical properties were used to characterize the joints.

2. Experimental procedure

2.1. Raw materials

The silicon nitride ceramic used was a sintered reaction bonded (Ceralloy 147-3N, Ceradyne) containing between 7 and 8 wt.% Y_2O_3–Al_2O_3 as sintering additive. Discs of 3 mm thick were cut from the initial rods (100 mm × 8 mm diameter) using a diamond cut-off wheel. All discs were polished down to 1 μm using diamond paste. The active brazing alloy (ABA) was produce by a successive electroless plating depositions on the surface of fine titanium powder [11]. The chemical composition was adjusted by the thickness of the coating. The final composition of the composite powder was 75 wt.% Cu–25 wt.% Ti. The iron aluminide alloy (FA-129) was supplied by CANMET in plate 15 cm wide by 25 cm in length (6.25 mm in thickness). The chemical composition of the intermetallic alloy is as follows: 16.6 Al, 4.67 Cr, 1.14 Nb, 0.027 C, and Fe bal. (wt.%). Discs of 8 mm in diameter by 3 mm in thickness were machined and polished down to 1 μm. Cu interlayers were punched from a 300 μm thick foil. The thickness was adjusted through grinding and polishing to a thickness of 200 μm. Both surfaces were polished down to 1 μm using Al_2O_3.

The sample configuration for microscopic evaluation was Si_3N_4/ABA/Cu/ABA/FA-129. The applied thickness of the filler metal in paste form was approximately 50 μm. The same configuration was used for the mechanical tests except that another Si_3N_4/FA-129 interface was used on the other end of the test specimen producing a sandwich sample Si_3N_4/Cu/FA-129/Cu/Si_3N_4. In both cases, all the components were cleaned in acetone in an ultrasonic bath prior to assembly.

2.2. DSC experiments

The independent and combined reactions involved at the interface of the Si_3N_4/Cu interlayer was characterized using differential scanning calorimetry (Netzsch DSC 404-C). Comparison of the melting of; ABA, a mixture of ABA and Cu powder (50–50 vol.%), a mixture of ABA and Si_3N_4 powders (30–70 vol.%) and a mixtures of ABA, Cu, and Si_3N_4 powders (39–31–30 vol.%) was conducted under a heating rate of 40 °C/min. The alumina crucible was lined with Nb foil to avoid contact between ABA and the crucible (a major exothermic peak would otherwise occur when Ti from the molten ABA reacts with Al_2O_3). All experiments were carried out in flowing high purity argon.

2.3. Bonding procedure

The sample was inserted in a graphite die surrounded by BN powder in a controlled atmosphere graphite furnace. A static pressure of 300 kPa was applied to the sample and was maintained throughout all tests. The furnace was heated to the soaking temperature at a heating rate of 10 °C/min and then cooled at 5 °C/min. The soaking temperatures studied were 925, 975, and 1025 °C for holding times of 1, 3, 6, and 12 min, respectively. Flowing argon was used during all the joining cycles.

2.4. Microscopic evaluation

Selected samples were cut, mounted and polished for microscopic evaluation. A light optical microscope with an image analysis system (Nikon; CLEMEX System), an SEM coupled with an EDS system (JEOL-840/EDAX), and a low voltage SEM coupled with an EDS detector (Hitachi S-4700/Oxford) were used to characterize the joints.

2.5. Mechanical properties

Four-point bending tests were performed using longer sandwich samples. Each ceramic bar was 2.5 cm in length instead of 3 mm as for microstructural evaluation samples. Testing was performed at room temperature on a universal testing machine (Tinius Olsen H25K-5) using a cross-head speed of 0.5 mm/min. The inner and outer span distances were, respectively, 20 and 40 mm. Each value reported is the average of three tests.

3. Results

3.1. Joint simulation in DSC

Differential scanning calorimetry (DSC) was used to identify the melting and reaction sequences of the active brazing powder with the various components in the joint. Fig. 1 presents four DSC traces; melting of ABA powder, melting of ABA in the presence of copper, melting and reaction of ABA with Si_3N_4 and melting of ABA in presence of copper and Si_3N_4, respectively. Each of these tests was performed under the same conditions.

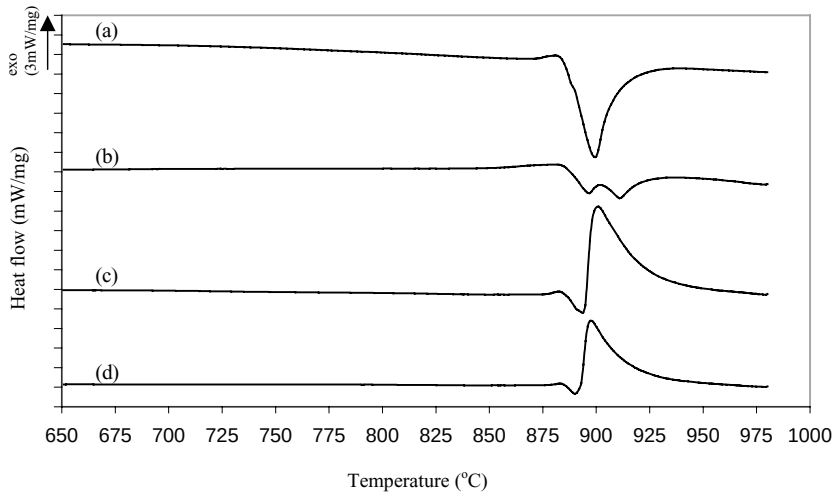

Fig. 1. Four DSC traces; (a) melting of single ABA powder, (b) melting of ABA in presence of copper, (c) melting and reaction of ABA with Si_3N_4, and (d) melting of ABA in presence of copper and Si_3N_4.

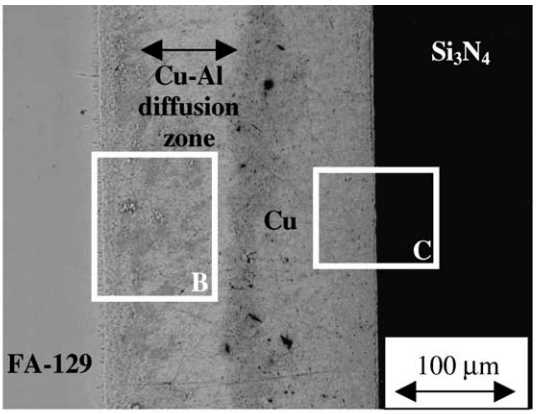

(a)

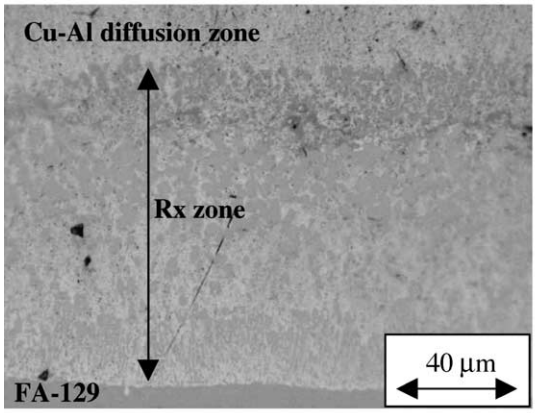

(b)

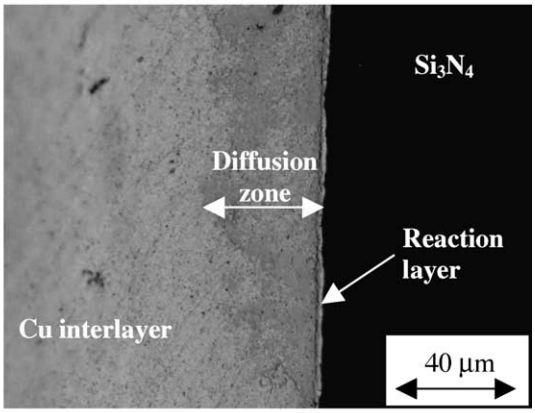

(c)

Fig. 2. Optical micrograph of (a) a complete interface, (b) the FA-129/Cu interface, and (c) the interface Cu/Si_3N_4.

- Trace 1: The melting of the filler metal occurs in one single event, between 886 and 915 °C. As the powder is composed of the Cu–Ti diffusion couple, melting initiates in the core of the powder, more specifically in the Cu_4Ti–Cu_3Ti_2 two-phase region (copper-rich eutectic [12]). Melting was observed at a temperature slightly higher than the reference temperature of the phase diagram as heating occurred in non-equilibrium conditions. The energy absorbed for the complete melting of the powder is −114 J/g.
- Trace 2: In the presence of copper powder, a dilution effect should be observed. In such case, the melting occurs in two stages. Melting also starts at 886 °C but an exotherm starting at 894 °C is also observed. The mixture starts to absorb energy again and the second endotherm is observed at 905 °C. This suggests solidification by dissolution of Cu from the pure powder to the reactive liquid up to its maximum solubility and re-melting of the powder as the temperature of the furnace reaches the liquidus of the powder. The overall energy for the melting event in the presence of copper decreases to −54 J/g.

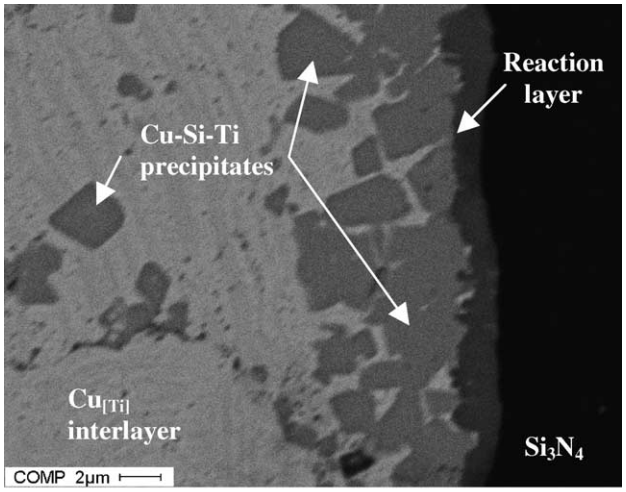

(a)

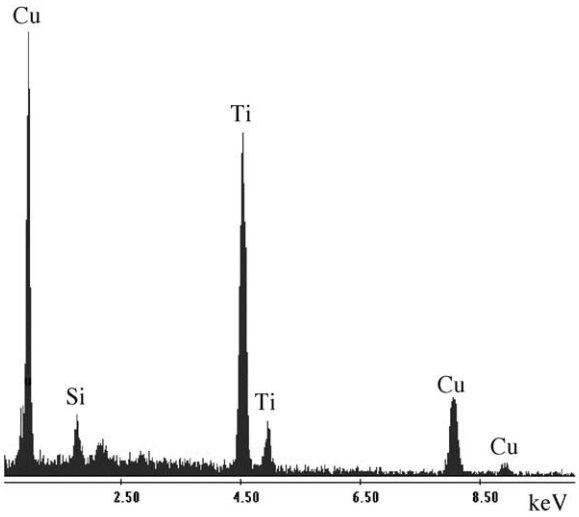

(b)

Fig. 3. (a) Back-scattered micrograph of a Si_3N_4/Cu interface and (b) EDS analysis of the precipitate identified in (a) respectively.

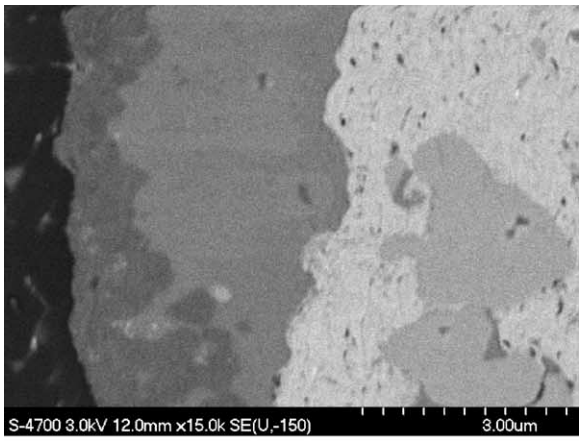

(a)

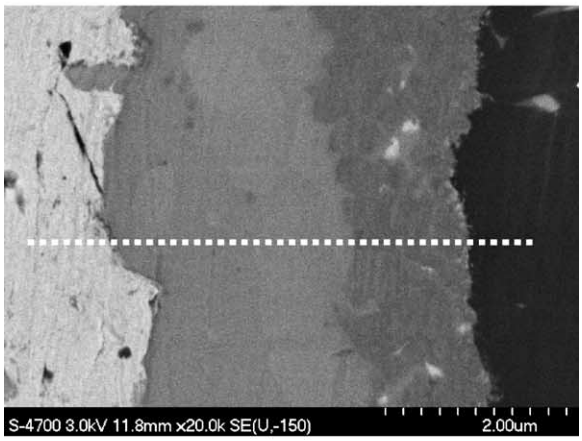

(b)

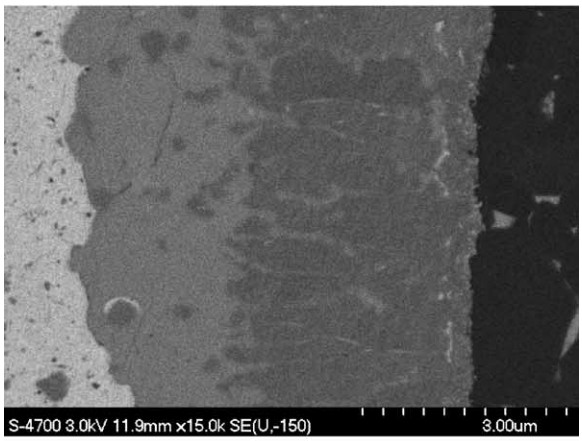

(c)

Fig. 4. Back-scattered micrographs of the interface between the Si_3N_4 and the Cu interlayer for sample brazed at (a) 975 °C for 1 min, (b) 1025 °C for 1 min, and (c) 1025 °C for 12 min.

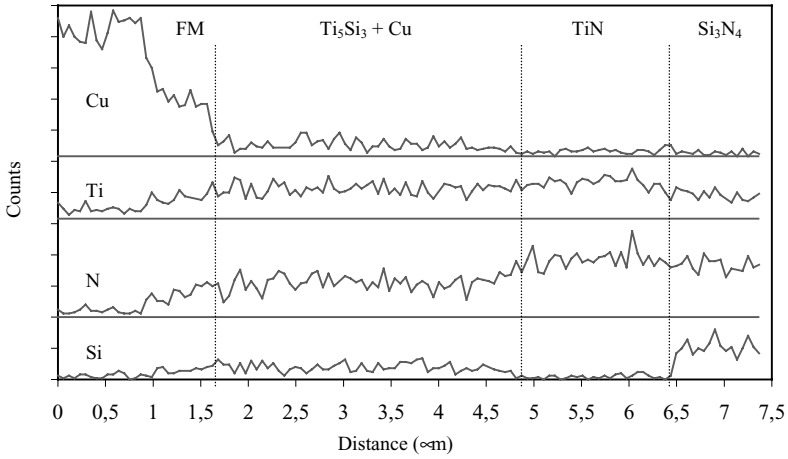

Fig. 5. Low voltage line scan of the reaction layer observed in Fig. 4b.

- Trace 3: The third curve presents the reaction behavior between the active brazing alloy and Si_3N_4 powder. Melting of the filler metal begins and initiation of the reaction between Ti and Si_3N_4 starts before complete melting of the ABA powder occurs. This suggests that molten active liquid has reached the surface of the powder and come in contact with the ceramic powder. The temperature where this exotherm starts is 894 °C. This temperature is identical to the temperature where the first exotherm begins in the case of ABA–Cu mixtures. The total melting and reaction energy in this case is +141 J/g. The annihilation of the melting peak is due to the high energy released during the reaction between Ti and Si_3N_4 to form TiN and Ti_5Si_3.
- Trace 4: The last trace describes the simulation of a joint comprising Si_3N_4/ABA/Cu. A similar behavior to that for the sample Si_3N_4/ABA was observed; initiation of melting and reaction with the ceramic when the active liquid reaches the surface. However, the presence of copper has an effect on the energy released by the reaction as competition between dilution (solidification) and reaction occurs. The simulation of a joint formation shows a complete melting and reaction energy of +100 J/g, indicating the effect of ABA dilution by Cu.

3.2. Microstructural analysis

Fig. 2 presents representative optical micrographs of: (a) the complete joint, (b) the interface between the FA-129 and the Cu interlayer and (c) the interface between the Cu interlayer and the silicon nitride ceramic. The sample was brazed at 975 °C for 6 min. Two different types of reaction are occurring simultaneously on both sides of the Cu interlayer. At the FA-129/Al interface, the characteristic copper color was not found but a yellow layer is presents (under the optical microscope). This layer is a solid solution of copper and aluminum formed by diffusion of aluminum from the iron aluminide alloy into the active brazing alloy. In addition, the presence of molten ABA in contact with the iron aluminide produces a reaction zone (100 μm in this case), where the thickness is a function of brazing temperature and time. However, the morphology of the reaction layer is similar and only the thickness changes. The Cu/Si_3N_4 interface shows the formation of a reaction layer at the surface of the ceramic and the diffusion of the excess of ABA into the Cu interlayer. A zone possessing the characteristic copper color between both diffusion zones is observed, suggesting that the complete interlayer has not been affected by diffusion.

3.2.1. Si_3N_4/Cu interface characterization

Fig. 3a presents a general back-scattered micrograph of the Cu/Si_3N_4 interface of a sample brazed at 925 °C for 12 min. In addition to the reaction layer, another type of precipitate is observed close to the reaction layer. The EDS spectrum of this phase is presented in Fig. 3b. The main peaks detected are Cu, Si, and Ti. The Cu–Ti–Si phase is in contact with the reaction layer in some locations. These precipitates are observed up to a distance of 70 μm from the interface.

Fig. 4 presents back-scattered micrographs of the interface between the Si_3N_4 and the Cu interlayer for samples

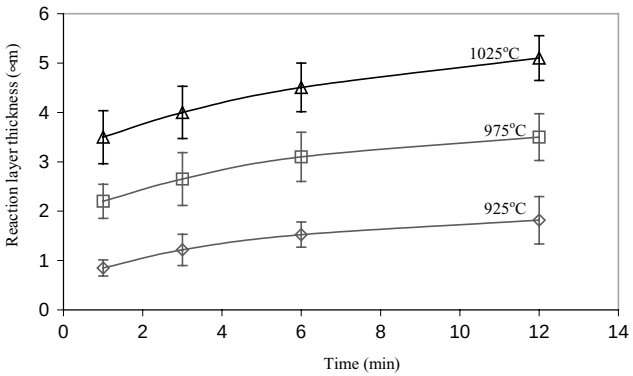

Fig. 6. Reaction layer thickness as a function of brazing parameters.

brazed at (a) 975 °C for 1 min, (b) 1025 °C for 1 min, and (c) 1025 °C for 12 min. Fig. 5 presents the low voltage line scan of the interface shown in Fig. 4b (dashed line). In all three cases, the interface is composed of two layers possessing similar atomic number composition, independent of the joining conditions. The joining conditions do, however, affect the relative thickness of both components of the reaction layer. The low voltage line scan indicates a layer rich in Ti and N adjacent to the interface of the ceramic and a layer rich in Ti and Si and containing Cu next to this layer. The Ti and N-rich layer is believed to be TiN and the Ti–Si is believed to be a Ti_5Si_3 compound containing a certain level of Cu in solution. The effect of temperature on the morphology of the layer shows that both layers grow and the thickness ratio between the TiN layer and the total reaction layer thickness slightly increases with increasing temperature. However, the effect of time at high temperature definitely shows a significant increase in the TiN layer with respect to the total reaction layer. Si has been detected in the filler metal and its concentration decreases further from the reaction layer. The similarity between the Ti and N line scan is produced by the convolution of the X-rays peaks (Ti Lα and N Kα). As the reaction layer growth is a more complex phenomenon than a single reaction system—due to evidence of growth competition between the different reactions—the total reaction layer thickness was measured as a function of brazing parameters and the results are presented in Fig. 6. The reaction layer thickness ranges between 0.85 and 5.1 μm. In all three cases, the data fits the final part of a parabolic trend, suggesting that the growth follows a diffusion controlled type of reaction. In addition, the fit suggests that in all cases, the growth rate is diminishing to zero, indicating that the reaction layer is not growing fast with respect to time.

The parabolic growth law was firstly applied to the reaction layer growth data obtained and the results are presented in Fig. 7a. In all three cases, the linear fit is in strong agreements with the experimental measurements. None of the trend lines in Fig. 7a pass through the origin, implying that even for very short joining conditions, the solid–liquid reaction is completed (the reaction layer completely covers the Si_3N_4 ceramic surface) and a diffusion process is now controlling the further growth of the layer. The good fit of the linear behavior suggests that the parabolic equation is valid for this case and that other more complex analyses and models such as the Jonhson–Mehl equation are not necessary [13]. The effective activation energy calculated for the layer growth is 137 kJ/mol and the plot is presented in Fig. 7b.

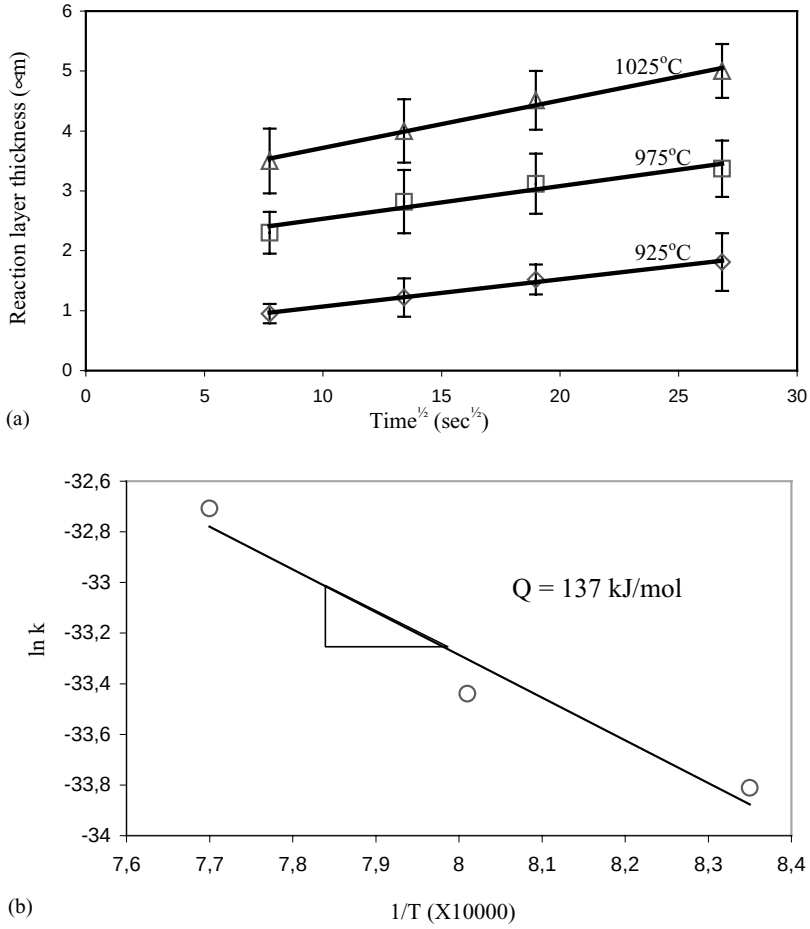

Fig. 7. Modeling of the reaction layer growth by (a) parabolic analysis and (b) activation energy measurement with Arrhenius equation.

3.2.2. Cu/FA-129 interface characterization

Fig. 8a presents a back-scattered micrograph of the iron aluminide alloy very close to the Cu/FA-129 interface for a joint brazed at 975 °C for 3 min. The remainder of the FA-129 bulk material are observed on the left hand side. Cu diffusion in the iron aluminide structure is observed as small bright dots. The iron aluminide alloy presents a wavy interface, suggesting dissolution into the molten active metal. Some precipitates are formed close to the iron aluminide dissolution zone. Two distinct compositions are observed and their respective EDS analysis are presented in Fig. 8b and c, respectively. The darker precipitates are Ti-based and the brighter ones are Fe-based. All the precipitates formed are surrounded by a Cu–Al alloy.

Fig. 9a presents a back-scattered montage of the complete interface between the FA-129 alloy and the Cu interlayer brazed at 975 °C for 3 min. The EDS analysis of the bigger precipitates is presented in Fig. 9b. The chemical analysis of the Ti-based precipitates is similar, independent of the distance from the FA-129 bulk material. The micrograph shows that the Fe-based precipitates are only observed near the interface and that the Ti-based precipitates are present at a greater distance form the interface. The Ti-based precipitates are believed to be formed from a combination of the Ti from the active brazing alloy and slight dissolution of the Fe_3Al intermetallic in the Cu–Al molten liquid. Fig. 9c presents the EDS analysis of the Cu–Al matrix and shows that at distances over 100 μm, Al is still present.

3.3. Mechanical properties

Fig. 10 presents the results of the four-point bending tests performed on the joint as a function of the reaction layer thickness. These samples were selected as they, within the error bars, represent a certain range of reaction layer thickness. Their respective joining conditions can be derived from Fig. 6. The strength increases with the reaction layer thickness. The peak value obtained is 160 MPa. In all cases,

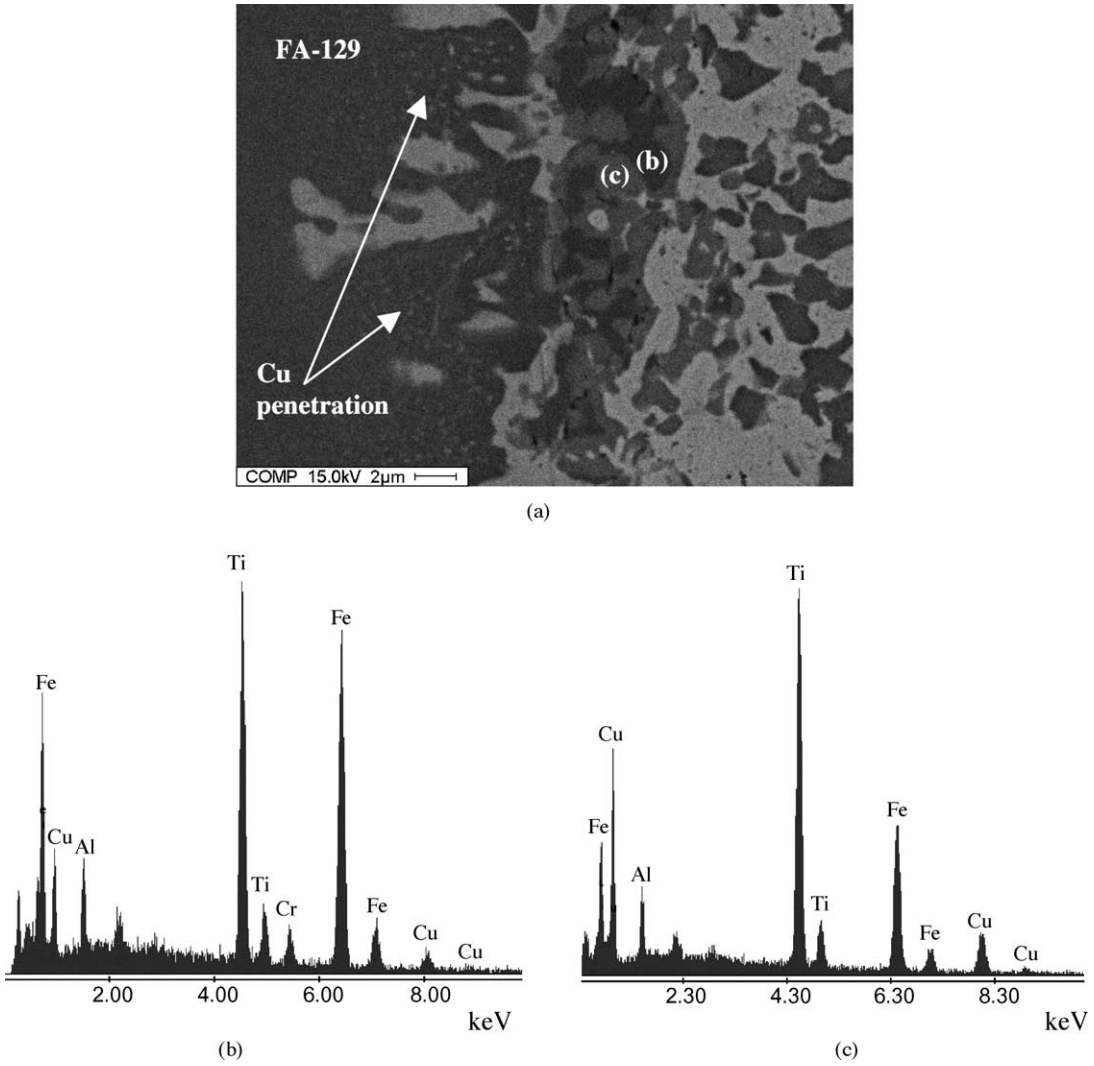

Fig. 8. (a) Back-scattered micrograph of the FA-129 very close to the Cu/FA-129 interface, (b) and (c) EDS analyses of two reactions products formed close to the intermetallic.

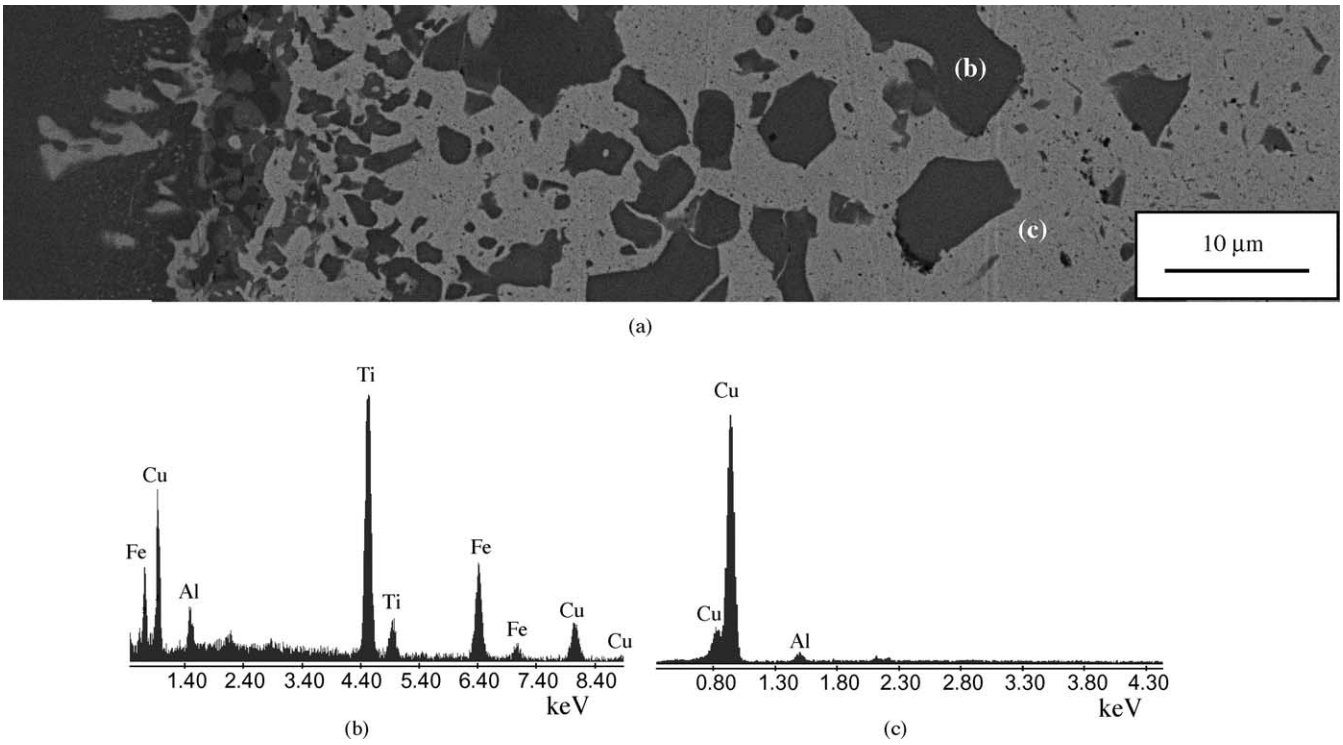

Fig. 9. (a) back-scattered montage of the FA-129/Cu interlayer interface, (b) EDS analysis of Ti precipitates, and (c) EDS analysis of Cu–Al matrix, respectively.

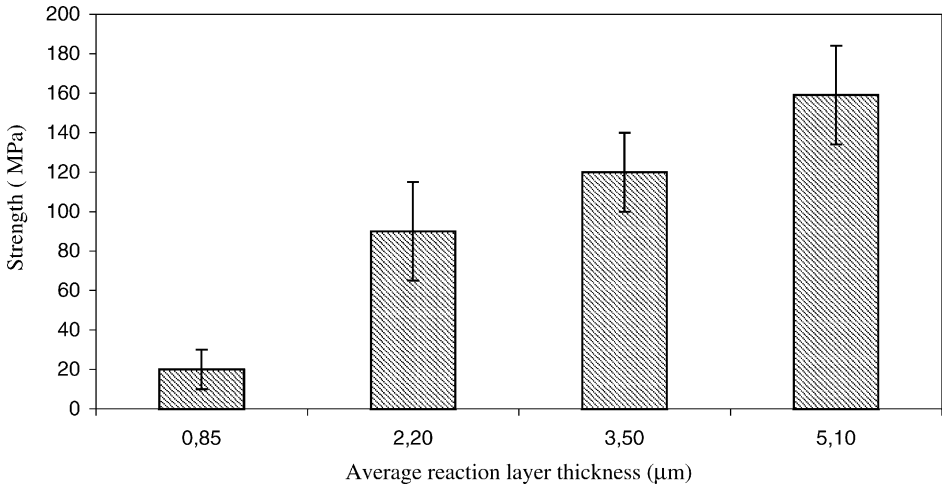

Fig. 10. Four-point bending strength of the joints as a function of reaction layer thickness.

the fracture occurs through the ceramic interlayer interface, suggesting that the reaction between the iron aluminide alloy and the Cu interlayer possesses a higher strength than 160 MPa.

4. Discussion

The copper interlayer has two main functions: (1) to reduce the residual stresses produced during cooling and (2) to dilute the active brazing alloy by titanium diffusion to obtain a better control on the reaction layer growth. At first, the insertion of the copper seems to have beneficial effects on the joint reliability as sound joints have been produced, as opposed to results obtained previously with direct brazing.

The microstructure formed at the ceramic/interlayer interface is mainly composed of a reaction layer, evolving with time and temperature. This reaction layer is composed of a bi-layer system of TiN and Ti_5Si_3 containing Cu. During

reaction between the Ti and the Si_3N_4, TiN, and Ti_5Si_3 are the most thermodynamically favorable compounds to be formed [14]. However, their respective growth is a function of the adjacent solute composition and the chemical interaction with the reaction layer. The dissolution of the Ti_5Si_3 layer in the filler metal also reduces the thickening. This is observed by the presence of precipitates containing Cu, Ti, and Si close to the reaction layer. The silicon content of these precipitates is obviously coming from the Si_3N_4, as its the only source of Si in the system. These precipitates are also present in higher quantity when the brazing temperature and time are increased.

The reaction competition is also influenced by the dilution of Ti in the copper interlayer as observed by DSC and modeling of the reaction layer growth. The DSC results show that copper powder reduces the fusion energy of the active brazing alloy by solidification. Moreover, the joint simulation shows clearly the effect of copper by reducing the fusion energy by 33%, compared with similar powder mixtures of Si_3N_4 powder and active brazing alloy. Modeling the reaction layer growth through the parabolic law gave an activation energy of 137 kJ/mol. This activation energy is slightly more than double the energy calculated for the system Si_3N_4/ABA/Si_3N_4 using the same starting materials [15]. The diffusion of titanium towards the copper interlayer reduces the availability near the reaction layer front and then slows the growth rate. The presence of Ti has been detected at more than 70 μm from the interface.

The interface between the FA-129 and the Cu interlayer is more complicated to explain as a series of reactions occur concurrently. The formation of a Cu–Al alloy from diffusion occurs simultaneously to the penetration of Cu into the iron aluminide alloy. Fe possesses a low solubility in pure copper but increases slowly in the molten stage. The presence of Ti is believed to increase the solubility of Fe in the filler metal but no phase diagrams are available to confirm this hypothesis. The variation in the composition of both precipitates should be related to the distance from the dissolution point as the precipitates rich in Fe are closer to the FA-129 and the Ti-rich precipitates, away from the interface, are formed by solidification of the filler metal in the presence of a trace concentration of Fe. Again, no phase diagrams are available to confirm this statement, however, the microstructural development appears to suggest this behavior.

The mechanical properties were tested as a function of their total interlayer thickness. From a reaction layer point of view, the maximum strength of the joints hardly increased above 160 MPa as the reaction layer growth rate slows down after 12 min for all conditions and the effect of time becomes a minor factor. To increase the reaction layer, an increment in the brazing temperature has to be used, but previous results have demonstrated that 1025 °C is nearly the maximum operating temperature for this system. Increasing the brazing time to 1025 °C showed significant growth of the TiN layer compared to the total reaction layer.

5. Conclusions

The benefits of inserting a Cu interlayer to absorb the residual stresses formed during cooling have been demonstrated. Sound joints between Si_3N_4 and FA-129 were achieved. The reaction layer at the Si_3N_4/Cu interface is composed of TiN and Ti_5Si_3. The total reaction layer thickness follows a parabolic growth behavior, but growth competition between the two components forming the reaction layer occurs, making detailed kinetic modeling impossible. The effective activation energy was calculated as 137 kJ/mol. Dissolution of the FA-129 occurs at the Cu interlayer interface and Al encountered to diffuse from the intermetallic into the filler metal. Fe-rich precipitates are found near the interface whereas Ti-rich precipitates are observed at distances of more than 100 μm from the interface. The mechanical properties have shown a maximum peak strength of 160 MPa.

Acknowledgements

The authors would like to acknowledge NSERC, Canada, for funding the project. The authors would also like to acknowledge NATEQ for the scholarship awarded to M. Brochu. The authors would also like to thank Dr. S.F. Corbin and Mr. D. Turriff for the utilization of the DSC.

References

[1] J. A Fernie, W.B. Hanson, Best practice for producing ceramic–metal bonds, Ind. Ceram. 19 (3) (1999) 172–175.
[2] K. Suganuma, Joining Non-Oxide Ceramics, Ceramics and Glasses, Engineered Materials Handbook, vol. 4, ASM International, 1991, pp. 523–531.
[3] Y.D. Huang, W.Y. Yang, Z.Q. Sun, Effect of the alloying element chromium on the room temperature ductility of Fe_3Al intermetallics, Intermetallics 9 (2001) 119–124.
[4] V.K. Sikka, C. T Liu, Iron–aluminide alloys for structural use, Mater. Technol. 9 (7/8) (1994) 159–162.
[5] M.G. Nicholas, Joining Processes Introduction to Brazing and Diffusion Bonding, Kluwer Academic Publishers, The Netherlands, 1998.
[6] S.D. Peteves, G. Ceccone, M. Paulasto, V. Stamos, P. Yvon, Joining silicon nitride to itself and to metals, J. Metals January (1996) 48–52, 74–77.
[7] T.W. Kim, S.W. Park, Effects of interface and residual stress on mechanical properties of ceramic/metal system, Key Eng. Mater. 183–187 (2000) 1279–1284.
[8] M. Brochu, M.D. Pugh, R.A.L. Drew, Microstructure evolution during brazing of silicon nitride to iron aluminide alloy using soft interlayer, in: M. Brochu, M.D. Pugh, R.A.L. Drew (Eds.), Proceeding of the Metal/Ceramic Interactions Symposium, COM 2002, CIM, Montreal, Canada, pp. 45–56.
[9] V.K. Sikka, in: A.K. Koul, et al. (Eds.), Development of Nickel and Iron Aluminides and their Applications, Advances in High Temperature Structural Materials and Protective Coatings, National Research Council of Canada, Ottawa, 1994, pp. 282–295.
[10] M. Brochu, M.D. Pugh, R.A.L. Drew, Active brazing of silicon nitride to iron aluminide alloy, in: Proceeding of the 10th International Ceramic Congress and Third Forum on New Materials, Florence, Italy, 14–18 July 2002, pp. 757–765.

[11] M. Brochu, M.D. Pugh, R.A.L. Drew, Active brazing alloy produced by electroless plating technique, Ceram. Eng. Sci. Proc. 23 (3) (2002) 801–808.
[12] ASM Handbook, vol. 3, Phases Diagrams, ASM International, USA.
[13] Y. Nakao, K. Nishimoto, K. Saida, Reaction layer formation in nitride ceramics (Si_3N_4 and AlN) to metals joints bonded with active filler metals, ISIJ Int. 30 (12) (1991) 1142–1150.
[14] R.E. Loehman, A.P. Tomsia, J.A. Pask, S.M. Johnson, Bonding mechanisms in silicon nitride brazing, J. Am. Ceram. Soc. 73 (3) (1990) 552–558.
[15] M. Brochu, M.D. Pugh, R.A.L. Drew, Joining silicon nitride ceramic using a composite powder as active brazing alloy, Mater. Sci. Eng. A, submitted for publication.